DOI: 10.1002/anie.201208320

Electroreduction

Selectivity of CO_2 Reduction on Copper Electrodes: The Role of the Kinetics of Elementary Steps**

Xiaowa Nie, Monica R. Esopi, Michael J. Janik, and Aravind Asthagiri**

Electrochemical reduction of CO_2 is a candidate process for energy storage and synthetic fuel production, and if selectivity to alcohols could be promoted, this process would allow for a synthetic sustainable carbon cycle using liquid fuels derived from sustainable electricity sources.[1–3] Cu electrodes, of all metals examined experimentally, have shown a unique ability to produce hydrocarbon products at reasonable currents and efficiencies, but with a still relatively large overpotential of approximately 1 V.[4] High overpotentials and poor understanding of the factors that affect the selectivity of Cu catalysts are significant barriers to application. The primary hydrocarbon products in CO_2 electroreduction on Cu are methane and ethylene with negligible methanol formation.[5–7] The production of methane instead of methanol for electroreduction conflicts with what is observed in heterogeneous gas-phase methanol synthesis from CO_2 or CO hydrogenation, where Cu-based catalysts are used to convert CO_2 or CO to methanol.[8] This raises a fundamental question as to the mechanism for CO_2 reduction on Cu electrodes, which is an area of intense debate.[5–7,9–12] Understanding the O–H, C–H bond forming steps, as well as the C–C coupling steps leading to alcohols and various hydrocarbon products on Cu electrodes would provide significant insights for the design of new electrocatalysts for this reaction and into similar efforts in (photo)electroreduction of CO_2.

Although several experimental electrokinetic studies of CO_2 reduction on various Cu catalysts have been undertaken,[4–6,9,11,13] the rate-limiting and key selectivity-determining steps are still controversial. Several groups have shown that CO reduction results in a similar product distribution and potential dependence as CO_2 reduction, thereby reinforcing that the rate-determining step occurs after CO formation.[9,14,15] Recent experimental work by Kuhl and co-workers suggests that the key intermediate leading to hydrocarbon products is an enol intermediate, but the exact intermediate has not been resolved.[7] Recently, Peterson and co-workers proposed a detailed reaction path for methane production from electroreduction of CO_2 on various Cu surfaces based on, to our knowledge, the first density functional theory (DFT) calculations.[10,16] Their proposed rate-limiting (overpotential-determining) step is the reduction of CO to formyl (CHO), which then converts to formaldehyde (CH_2O) and a methoxy species (CH_3O) through a series of reduction steps. Selectivity to methane over methanol is proposed to be determined in the final CH_3O reduction step. These DFT studies based on reaction free energies of elementary steps conflict with recent electrokinetic experiments by Schouten et al., where reduction of CH_2O directly produced methanol with methane as a minor side product.[6] Furthermore, electrokinetic experiments found that methane and ethylene share a common potential limiting step on the Cu(111) surface that is yet to be identified.[11] In total, these observations suggest that CH_2O and a CH_3O species are not intermediates in methane production, thus leaving the dominant reaction path and selectivity-determining step(s) for methane and ethylene production on Cu electrocatalysts still uncertain.

Herein, we present a systematic determination of the CO_2 electroreduction mechanism on Cu electrodes, including the rate-limiting and selectivity-determining steps. We present the first DFT study that examines the role of kinetics of elementary steps in CO_2 electroreduction, utilizing a newly developed approach to consider the rate of electron–ion transfer reactions. Computational models were constructed by explicitly incorporating the role of water in a computationally tractable manner, as shown in representative transition state structures in Figure 1. Our calculation results show that the preferred path for methane production determined solely based on reaction free energies is misleading, and reaction kinetics of elementary steps provide a different mechanistic explanation for methane/ethylene selectivity compared to methanol on Cu electrodes. We provide an alternative reaction path that explains both methane and ethylene production through a hydroxymethylidyne (COH) intermediate from CO reduction; this path reconciles the latest experimental results from the Koper research group[6,11] and is consistent with experiments on CO_2, CO, and CH_2O reduction on Cu electrodes.[5,6,9,11,14,15]

To evaluate electrokinetic rates of elementary steps with DFT methods, we have developed a simple approach to evaluate electrode-potential-dependent activation barriers.

[*] Dr. X. W. Nie, Prof. A. Asthagiri
William G. Lowrie Department of Chemical & Biomolecular Engineering, The Ohio State University
221A Koffolt Laboratories
140 West 19th Ave., Columbus, OH 43210 (USA)
E-mail: asthagiri.1@osu.edu
M. R. Esopi, Prof. M. J. Janik
Department of Chemical Engineering
Pennsylvania State University
104 Fenske Lab, University Park, PA 16802 (USA)
E-mail: mjanik@psu.edu

[**] We acknowledge the Ohio Supercomputing Center for providing the computational resources for this work. This work was supported by the Center for Atomic Level Catalyst Design, an Energy Frontier Research Center funded by the U.S. Department of Energy, Office of Science, Office of Basic Energy Sciences under Award Number DE-SC0001058.

Supporting information for this article is available on the WWW under http://dx.doi.org/10.1002/anie.201208320.

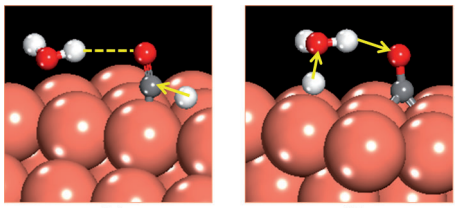

Figure 1. Electroreduction steps leading to the formation of a C–H bond occur through surface hydrogenation, as shown in the transition state (a) for CO reduction to CHO. O–H bond forming steps occur through H shuttling through water, as shown in the transition state (b) for CO reduction to COH. A more detailed picture of the entire path can be found in Figure S1 in the Supporting Information. Cu orange, O red, C gray, H white.

Representation of the electrified electrocatalytic interface within DFT models is challenging, and consideration of rates of coupled electron–ion transfer is especially difficult. The simple method applied here for inner-sphere electrocatalytic reactions was previously demonstrated to predict borohydride oxidation rates on a gold electrode that agreed well with experimental electrokinetics.[17] Coupled with the linear free energy method[18] for determining reaction free energies of elementary steps, we construct full reaction energy diagrams for CO_2 electroreduction on the Cu(111) surface. The method for activation barrier determination is described in more detail in the Supporting Information.

Based on previous experimental studies,[5–7,9,11,12] as well as DFT work by Peterson and co-workers,[10,16] possible reaction paths for production of methane (CH_4), methanol (CH_3OH), and ethylene (C_2H_4) on Cu(111) are proposed in Scheme 1. Though reduction may branch through many paths, a major branching point is whether CO is reduced to form a CHO or COH through formation of a C–H or O–H bond. We classify two major paths: path I through a CHO intermediate and path II through a COH intermediate, and examine these individually.

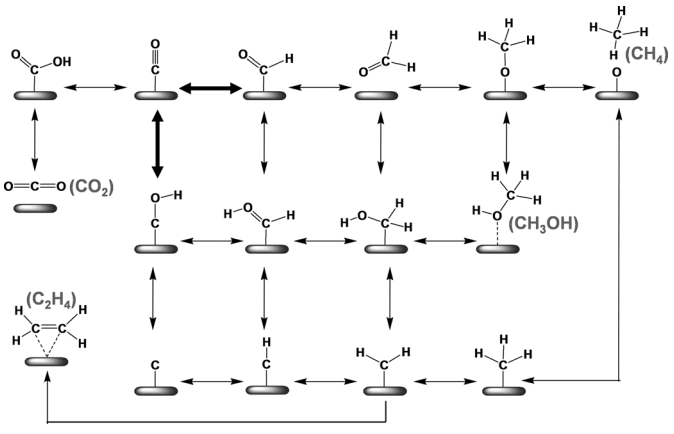

Scheme 1. Proposed reaction paths for CO_2 electroreduction on Cu(111), producing methane (CH_4), methanol (CH_3OH), and ethylene (C_2H_4). Electrochemical elementary steps for CH_4 and CH_3OH formation involve electron and proton transfer, whereas C_2H_4 is produced through nonelectrochemical CH_2 dimerization. $H^+ + e^-$ reactants and H_2O products are omitted.

Peterson and co-workers[10] proposed that methane is formed through a CHO intermediate, with the overall path proceeding as $CO_2 \rightarrow COOH \rightarrow CO \rightarrow CHO \rightarrow CH_2O \rightarrow CH_3O \rightarrow CH_4 + O \rightarrow CH_4 + OH \rightarrow CH_4 + H_2O$ (leaving off the $H^+ + e^-$ reactants and the first H_2O product formed). Methanol may be alternatively formed in the final step by CH_3O reduction, however, the elementary reaction producing methane was found to have a more favorable reaction free energy. While our free energy analysis of this path is similar to that of Peterson et al., the determination of kinetics of elementary steps changes the predicted product.

Activation barriers for all the elementary steps in path I were examined for both the water-solvated and H-shuttling models as shown in Figure 1, and are reported in Table S1 in the Supporting Information. We find that for all O–H bond formation reactions, including those also involving C–OH bond dissociation, the activation barrier is lower for the H-shuttling reaction. The polar O–H bond formation is stabilized through water-assisted proton shuttling coupled with electron transfer. For all C–H bond formation reactions, water-assisted H shuttling increases the activation barrier compared to direct hydrogenation from an adsorbed H* species. The less polar C–H bond requires direct surface interaction with both C and H at the transition state. The barriers have been evaluated for select steps in both path I and II with $2\,H_2O$ molecules, and are reported in Tables S1 and S3 in the Supporting Information.

Based on the evaluation of potential-dependent barriers, an electrode potential of approximately −1.15 V (RHE) is required to get the barriers in path I surmountable ($\leq$ 0.4 eV)[19] at room temperature (Figure S2 in the Supporting Information; RHE = reversible hydrogen electrode). At −1.15 V (RHE) the computed barrier for the final methanol production step is 0.15 eV, whereas methane production must overcome a barrier of 1.21 eV. The preferred transition states of methanol and methane formation from CH_3O reduction are shown in Figure 2. The high barrier for formation of methane is due to the structure of the adsorbed CH_3O species, which orients the O–C bond perpendicular to the surface. The CH_3O species must bend to reorient the C atom near the surface. C–H bond formation coupled with C–O dissociation in this reaction requires direct involvement of the metal surface, and as such is kinetically prohibitive. The selectivity ratio is 6×10^{17} for methanol over methane production through path I at room temperature. Path I produces solely methanol rather than methane, which is consistent with

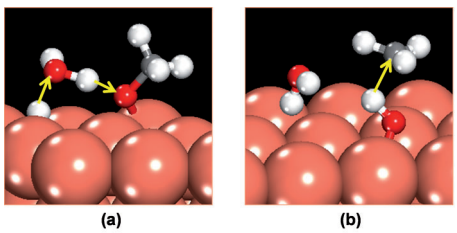

Figure 2. Transition states from reduction of surface methoxy species to produce a) methanol in the H-shuttling model, and b) methane in the water-solvated model. A more detailed picture of the entire path can be found in Figure S3 in the Supporting Information.

experimental observations that electroreduction of CH_2O on Cu dominantly gives methanol.[6] This result leaves as an open question: What is the reaction path to the experimentally observed methane and ethylene products on Cu electrodes?

Based on previous electrokinetic experiments,[9,12] we examined a possible reaction path II through a COH intermediate for methane production, which differs from path I beginning with CO reduction, following a path to methane of $CO \rightarrow COH \rightarrow C \rightarrow CH \rightarrow CH_2 \rightarrow CH_3 \rightarrow CH_4$ (leaving off the $H^+ + e^-$ reactants and H_2O products). Activation barriers for all the elementary steps in the preferred model for path II are given in Table S3 in the Supporting Information. According to the potential-dependent barriers for the elementary steps, an electrode potential of approximately −1.15 V (RHE) is also needed to get all the barriers surmountable (≤ 0.4 eV) at room temperature for path II (Figure S4 in the Supporting Information). Within path II, once COH is formed from CO reduction, it further reduces to an adsorbed C intermediate by forming an additional O–H bond and dissociating the product water. Observation of a graphitic carbon species was reported by DeWulf and co-workers based on X-ray photoelectron spectroscopy (XPS) and Auger electron spectroscopy (AES) performed in situ during CO_2 electroreduction experiments on Cu electrodes.[9] Once surface carbon is formed, it is reduced to CH, CH_2, and CH_3 over relatively low barriers.

Recently, Schouten et al. examined CO electroreduction on Cu(111) at pH 7 and reported the initial formation of methane and ethylene around −0.9 V (RHE).[11] Our onset-potential estimate is in reasonable agreement with this value, given the approximation of a 0.4 eV kinetic threshold. Our barrier is likely an upper bound, and other effects such as coverage and presence of defects (e.g. step edges even in nominally Cu(111) samples) could have effects on the onset of methane/ethylene production.

Both path I (producing methanol) and path II (producing methane) are kinetically feasible at potentials below approximately −1.15 V (RHE). Therefore, the key selectivity step between these two paths will be dictated by the relative preference of CO to reduce to CHO or COH. At −1.15 V (RHE), the activation barriers for CHO and COH formation from CO reduction are 0.39 and 0.21 eV, respectively (Figure 3). Owing to the difference of 0.18 eV in activation barrier, the COH path is favored by a selectivity factor of around 2000 at 300 K. The preference of COH formation from CO results in the experimentally observed selectivity to methane over methanol.

In the recent paper by Schouten et al. on formation of ethylene from CO reduction on single-crystal Cu electrodes, the path shared by methane and ethylene has a common intermediate and was found to take place preferentially at the Cu(111) facet.[11] To determine if our proposed path for methane shows a similar branching to ethylene, we examined the nonelectrochemical ethylene formation from dimerization of two CH_2 species on Cu(111). The effective barrier for ethylene formation is calculated to be 0.21 eV. This can be compared to the barrier for CH_2 reduction to CH_3, which varies from 0.55 eV at 0 V (RHE) to 0 eV at −1.15 V (RHE). Though the rate constant favors ethylene selectivity at lower overpotentials, the relative coverage of CH_2 and H will also affect the selectivity and might be expected to further promote methane formation at higher overpotentials. Hori and co-workers observed that methane production rises with increasing overpotentials as ethylene production levels off,[5] thus matching at least qualitatively the competitive behavior suggested by our DFT calculations.

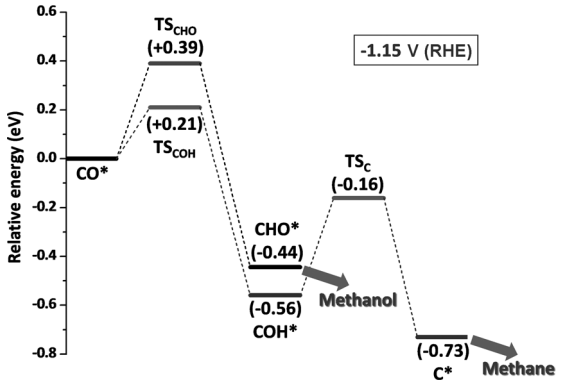

Figure 3. Relative energy diagrams for selectivity-determining steps in path I and path II, at −1.15 V (RHE). TS = transition state.

In conclusion, DFT calculations of the activation barriers of elementary steps have resolved that the reduction of CO is the key selectivity-determining step for CO_2 electroreduction on Cu(111). The dominant path proceeds through reduction of CO to COH, which eventually leads to CH_x species, and can produce both methane and ethylene. This path does not occur during the nonelectrochemical methanol synthesis from syngas owing in part to the lack of an aqueous environment to promote CO–H bond formation, but also because the applied potential is needed to drive the forward reaction through COH to methane/ethylene. Our proposed path is able to reconcile the experimental data on CO_2, CO, and CH_2O reduction on Cu electrodes. While other side reactions may still play a role, and coverage effects, step edges, Cu surface facet, and the role of additional solvation need to be explored in the future, this contribution makes a critical step forward in our fundamental understanding of CO_2 electroreduction on Cu surfaces. This analysis suggests that future design of heterogeneous catalysts for CO_2 (photo)electroreduction should focus on the relative energetics of COH versus CHO formation to tailor the selectivity of the desired products towards liquid fuels such as methanol.

Experimental Section

Methods

All calculations were performed within the framework of DFT, as implemented in the Vienna ab initio simulation program (VASP). Computational details are presented in the Supporting Information.

Received: October 16, 2012
Revised: January 9, 2013
Published online: January 23, 2013

Keywords: carbon dioxide · density functional calculations · heterogeneous catalysis · kinetics · renewable energy

[1] G. A. Olah, *Angew. Chem.* **2005**, *117*, 2692 – 2696; *Angew. Chem. Int. Ed.* **2005**, *44*, 2636 – 2639.
[2] G. A. Olah, A. Goeppert, G. K. S. Prakash, *J. Org. Chem.* **2009**, *74*, 487 – 498.
[3] D. T. Whipple, P. J. A. Kenis, *J. Phys. Chem. Lett.* **2010**, *1*, 3451 – 3458.
[4] Y. Hori in *Modern Aspects of Electrochemistry, Vol. 42* (Eds: C. G. Vayenas, R. E. White, M. E. Gamboa-Aldeco), Springer, New York, **2008**, pp. 89 – 189.
[5] Y. Hori, A. Murata, R. Takahashi, *J. Chem. Soc. Faraday Trans. 1* **1989**, *85*, 2309 – 2326.
[6] K. J. P. Schouten, Y. Kwon, C. J. M. van der Ham, Z. Qin, M. T. M. Koper, *Chem. Sci.* **2011**, *2*, 1902 – 1909.
[7] K. P. Kuhl, E. R. Cave, D. N. Abram, T. F. Jaramillo, *Energy Environ. Sci.* **2012**, *5*, 7050 – 7059.
[8] M. Behrens, F. Studt, I. Kasatkin, S. Kuhl, M. Havecker, F. Abild-Pedersen, S. Zander, F. Girgsdies, P. Kurr, B. L. Kniep, M. Tovar, R. W. Fischer, J. K. Norskov, R. Schlogl, *Science* **2012**, *336*, 893 – 897.
[9] D. W. Dewulf, T. Jin, A. J. Bard, *J. Electrochem. Soc.* **1989**, *136*, 1686 – 1691.
[10] A. A. Peterson, F. Abild-Pedersen, F. Studt, J. Rossmeisl, J. K. Norskov, *Energy Environ. Sci.* **2010**, *3*, 1311 – 1315.
[11] K. J. P. Schouten, Z. S. Qin, E. P. Gallent, M. T. M. Koper, *J. Am. Chem. Soc.* **2012**, *134*, 9864 – 9867.
[12] Y. Hori, R. Takahashi, Y. Yoshinami, A. Murata, *J. Phys. Chem. B* **1997**, *101*, 7075 – 7081.
[13] C. W. Li, M. W. Kanan, *J. Am. Chem. Soc.* **2012**, *134*, 7231 – 7234.
[14] M. Gattrell, N. Gupta, A. Co, *J. Electroanal. Chem.* **2006**, *594*, 1 – 19.
[15] Y. Hori, A. Murata, R. Takahashi, S. Suzuki, *J. Am. Chem. Soc.* **1987**, *109*, 5022 – 5023.
[16] W. J. Durand, A. A. Peterson, F. Studt, F. Abild-Pedersen, J. K. Norskov, *Surf. Sci.* **2011**, *605*, 1354 – 1359.
[17] G. Rostamikia, A. J. Mendoza, M. A. Hickner, M. J. Janik, *J. Power Sources* **2011**, *196*, 9228 – 9237.
[18] J. K. Nørskov, J. Rossmeisl, A. Logadottir, L. Lindqvist, J. R. Kitchin, T. Bligaard, H. Jonsson, *J. Phys. Chem. B* **2004**, *108*, 17886 – 17892.
[19] L. J. L. Häller, M. J. Page, S. A. Macgregor, M. F. Mahon, M. K. Whittlesey, *J. Am. Chem. Soc.* **2009**, *131*, 4604 – 4605.

